

Cite this: *Dalton Trans.*, 2019, **48**, 15521

Ionic-liquid-based synthesis of tellurium–rhenium carbonyls with specific reaction control†‡

Silke Wolf  and Claus Feldmann *

The novel tellurium rhenium carbonyls $[\text{Te}_2\text{Re}(\text{CO})_5][\text{AlCl}_4]$ (**1**), $[\text{BMIm}][\text{Te}_2\text{I}_4(\mu\text{-I})_2\text{Re}(\text{CO})_4]$ (**2**), $\{\text{Te}_3\}_2(\mu\text{-I})_3(\mu_3\text{-I})\text{Re}(\text{CO})_3$ (**3**) and $[\text{BMIm}][(\text{Te}_2)_3\{\text{Re}(\text{CO})_3\}_2\{\text{Re}(\text{CO})_4\}_3]$ (**4**) were prepared by reacting TeI_4 and $\text{Re}_2(\text{CO})_{10}$ in ionic liquids (ILs). $[\text{Te}_2\text{Re}(\text{CO})_5][\text{AlCl}_4]$ (**1**) was obtained in a mixture of $[\text{BMIm}]\text{Cl}$ (BMIm : 1-butyl-3-methylimidazolium) and AlCl_3 (ratio: 1 : 1) and contains a $[\text{Te}_2\text{Re}(\text{CO})_5]^+$ cation. Increasing the amount of AlCl_3 ($[\text{BMIm}]\text{Cl} : \text{AlCl}_3 = 1 : 2$) results in $[\text{BMIm}][\text{Te}_2\text{I}_4(\mu\text{-I})_2\text{Re}(\text{CO})_4]$ (**2**) with the anion $[\text{Te}_2\text{I}_4(\mu\text{-I})_2\text{Re}(\text{CO})_4]^-$. At a $[\text{BMIm}]\text{Cl}$ to AlCl_3 ratio of 1 : 3, $\{\text{Te}_3\}_2(\mu\text{-I})_3(\mu_3\text{-I})\text{Re}(\text{CO})_3$ (**3**) was realized with a Te_3I_3 ring and μ_3 -coordinating iodine. Finally, $[\text{BMIm}][(\text{Te}_2)_3\{\text{Re}(\text{CO})_3\}_2\{\text{Re}(\text{CO})_4\}_3]$ (**4**) was prepared in $[\text{BMIm}][\text{OTf}]$ (OTf : triflate) and contains the ufosan-like anion $[(\text{Te}_2)_3\{\text{Re}(\text{CO})_3\}_2\{\text{Re}(\text{CO})_4\}_3]^-$ with three Te_2^{2-} and two $\text{Re}(\text{CO})_3^+$ units that establish a distorted heterocuban-like cage. The compounds were characterized by single-crystal structure analysis, energy dispersive X-ray (EDX) analysis, thermogravimetry (TG), and infrared spectroscopy (FT-IR). The course of the reaction and the formation of the four novel tellurium-rhenium carbonyls can be directly correlated to the reaction conditions and especially to the acidity of the IL.

Received 7th May 2019,
Accepted 9th July 2019

DOI: 10.1039/c9dt01897b

rsc.li/dalton

Introduction

Due to their high redox stability, ionic liquids (ILs) turned out as suitable reaction media for the synthesis of metal clusters and reactive carbonyl compounds.^{1–4} A fascinating structure, for instance, relates to the guest-free germanium clathrate $\square_{24}\text{Ge}_{136}$ (\square indicates non-occupied lattice sites) representing a novel element modification of germanium.⁵ In view of carbonyls, especially compounds that are neither electronically nor sterically stabilized by alkyl or aryl ligands were obtained by IL-based synthesis. Such non-stabilized carbonyls were denoted as extremely labile and highly sensitive.⁶ Carbonyls without alkyl/aryl stabilization but with even more destabilizing halide ligands were actually considered as non-producible. Here, ILs reveal their full potential as they are exactly suitable to prepare such reactive carbonyl compounds.^{2,3} Beside excellent redox stability, the weakly coordinating properties and the stabilization *via* inherent cation–anion interactions turned out as further merits of ILs.^{1–4} By now, however, many IL-based syntheses predominately remain explorative and without

specific IL-based control and variability of the resulting compound. Only recently, first attempts to understand the decisive reaction parameters and studies to steer the course of the reaction were reported.⁴ Especially, Lewis-acidic ILs such as $[\text{Cation}][\text{AlX}_4]$ ($X = \text{Cl}, \text{Br}$) seem to allow specific control over the product composition.^{4,7,8}

Based on our previous studies, we could already realize several novel, reactive carbonyl compounds such as the adamantane-like Fe_4Sn_6 cluster in $[\{\text{Fe}(\text{CO})_3\}_4\{\text{SnI}_6\text{I}_4\}]^{2-}$,⁹ the ufosane-like Te_6Mn_2 in $[(\text{Te}_2)_3\{\text{Mn}(\text{CO})_3\}_2\{\text{Mn}(\text{CO})_4\}_3]^-$,¹⁰ or the anti- $(\text{WCl}_2)_6$ -type anion $[(\text{Pb}_6\text{I}_8)\{\text{Mn}(\text{CO})_5\}_6]^{2-}$.¹¹ All of them were prepared *via* IL-based synthesis. Aiming at novel carbonyls, we have yet addressed the system $\text{TeI}_4/\text{Re}_2(\text{CO})_{10}$. Here, all already known compounds are essentially stabilized by organic ligands. $\text{Re}(\text{CO})_3\{\text{TeIPh}\}_3(\mu_3\text{-I})$,¹² for instance, exhibits a central Re atom that is distorted octahedrally coordinated by three Te atoms and three CO ligands. Additionally, Te is connected to iodine and phenyl (Ph) ligands. $\text{IRe}(\text{CO})_4\text{Te}(\text{CH}_3)_2$, $\text{Re}(\text{CO})_3\text{I}(\text{TePh}_2)_2$ and $\{\text{Re}(\text{CO})_3\text{I}\}_2\text{Te}_2\text{Ph}_2$ also exhibit Te–Re bonds with iodine coordinated to Re.¹³ Furthermore, several compounds contain Te–Re–Te or Re–Te–Re strings.^{13b,c,14} Some examples exhibit four-membered Te_2Re_2 rings such as in $[\{\text{Re}(\text{CO})_4\}_2\{\mu\text{-TePh}\}_2]$.¹⁵ Few more sophisticated arrangements were described, including a trigonal planar Te with three $\text{Re}(\text{CO})_5$ units in $[\text{Te}\{\text{Re}(\text{CO})_5\}_3][\text{BF}_4]$ ¹⁶ or two $\text{Re}(\text{CO})_3$ groups bridged by three Te atoms in $[\{\text{Re}(\text{CO})_3\}_2(\mu\text{-TePh})_3]^-$.¹⁷ Finally, the largest Te–Re arrangements were reported for the distorted

Institute of Inorganic Chemistry, Karlsruhe Institute of Technology (KIT), Engesserstraße 15, 76131 Karlsruhe, Germany. E-mail: claus.feldmann@kit.edu

† Dedicated to Professor Annie K. Powell on the occasion of her 60th birthday.

‡ Electronic supplementary information (ESI) available. CCDC 1913799–1913802.

For ESI and crystallographic data in CIF or other electronic format see DOI: 10.1039/c9dt01897b



heterocubane $[\text{Re}_4\text{Te}_4(\text{CN})_{12}]^{4-}$,¹⁸ as well as for $(\text{Cp}^*)_3\text{Re}_3\text{Te}_8$,¹⁹ $[\text{Re}_6\text{Te}_8(\text{CN})_6]^{4-}$,²⁰ or $[\text{Re}_6\text{Te}_8(\text{TeI}_2)]\text{I}_2$,²¹ in which Re_6 octahedra are capped by Te atoms.

For the first time, we here use IL-based synthesis to study the system $\text{TeI}_4/\text{Re}_2(\text{CO})_{10}$. As a result, four new Te–Re carbonyl compounds can be identified, including $[\text{TeI}_2\text{Re}(\text{CO})_5][\text{AlCl}_4]$ (**1**), $[\text{BMIm}][\text{Te}_2\text{I}_4(\mu\text{-I})_2\text{Re}(\text{CO})_4]$ (**2**), $\{\text{Te}_3\text{I}_2(\mu\text{-I})_3(\mu_3\text{-I})\}\text{Re}(\text{CO})_3$ (**3**), and $[\text{BMIm}][(\text{Te}_2)_3\{\text{Re}(\text{CO})_3\}_2\{\text{Re}(\text{CO})_4\}_3]$ (**4**). In addition to the identification of the novel compounds, specific control of the resulting carbonyl is possible depending on the anion and acidity of the applied IL.

Results and discussion

$[\text{TeI}_2\text{Re}(\text{CO})_5][\text{AlCl}_4]$ (**1**)

$[\text{TeI}_2\text{Re}(\text{CO})_5][\text{AlCl}_4]$ was prepared by reacting TeI_4 and $\text{Re}_2(\text{CO})_{10}$ in a mixture of $[\text{BMIm}]\text{Cl}$ and AlCl_3 at 1 : 1 ratio. The synthesis results in red crystals of **1** with two minor by-phases: colorless crystals of excess $\text{Re}_2(\text{CO})_{10}$ and yellow needles of $[\{\text{Re}(\text{CO})_5\}_2\text{I}][\text{Al}_2\text{Cl}_7]$. The presence of $[\{\text{Re}(\text{CO})_5\}_2\text{I}][\text{Al}_2\text{Cl}_7]$ was validated by crystal structure analysis (ESI: Table S1 and Fig. S1, S2†), cation and anion, however, are well-known with, e.g., $[\{\text{Re}(\text{CO})_5\}_2\text{I}]^+$ in $[\{\text{Re}(\text{CO})_5\}_2\text{I}][\text{AsF}_6]$.²² **1** crystallizes with monoclinic symmetry in $P2_1/c$ and contains $[\text{TeI}_2\text{Re}(\text{CO})_5]^+$ cations and $[\text{AlCl}_4]^-$ anions (Table 1 and Fig. 1a). By compari-

son with similar compounds, an oxidation of Re^0 to Re^{+1} and a reduction of Te^{+IV} to Te^{+II} seems reasonable.¹³ Accordingly, the synthesis can be rationalized by the following equation:



Beside single crystal structure analysis, the composition of **1** was verified by EDX analysis. The observed Te : I : Re ratio of 0.87 : 2 : 0.63 (scaled on I) fits well with expected ratio (1 : 2 : 1).

The $[\text{TeI}_2\text{Re}(\text{CO})_5]^+$ cation exhibits Te–Re distances of 275.9(1) (Re1–Te1) and 275.7(1) pm (Re2–Te2) (Fig. 2a). These distances are very similar to those in **2**, **3**, **4** and also compare to literature data, e.g., 275.5–276.3 pm in $\text{Re}(\text{CO})_3\{\text{TeIC}_6\text{H}_5\}_3(\mu_3\text{-I})$ ¹² or 272.9–274.1 pm in $[\text{Re}(\text{CO})_3\text{Cl}\{o\text{-C}_6\text{H}_4(\text{TeMe})_2\}]$ (Table 2).¹⁴ In comparison to $[\text{Re}_6\text{Te}_8(\text{TeI}_2)]\text{I}_2$,²¹ in which TeI_2 units are coordinated to each Re atom of a Re_6 octahedron (Te–Re 266.4–267.2 pm), the distances in the title compound are slightly longer, which can be ascribed to the different bonding situation and valence state of Re. Furthermore, the Te atom is coordinated like a distorted trigonal pyramid and exhibits two Te–I bonds with distances of 269.4(2) (Te2–I3) to 272.6(2) pm (Te2–I4) in addition to the Te–Re bond and the remaining lone pair. Again, these distances fit well with literature, e.g., 275.4–278.8 pm for terminally bond I atoms in the Te_4I_{16} building unit of TeI_4 .²³

Table 1 Crystallographic and refinement details of $[\text{TeI}_2\text{Re}(\text{CO})_5][\text{AlCl}_4]$ (**1**), $[\text{BMIm}][\text{Re}(\text{CO})_4\text{Te}_2\text{I}_4(\mu\text{-I})_2]$ (**2**), $\text{Re}(\text{CO})_3\{\text{Te}_3\text{I}_2(\mu\text{-I})_3(\mu_3\text{-I})\}$ (**3**) and $[\text{BMIm}][(\text{Te}_2)_3\{\text{Re}(\text{CO})_3\}_2\{\text{Re}(\text{CO})_4\}_3]$ (**4**)

| Data | 1 | 2 | 3 | 4 |
|---------------------------------|--|---|---|---|
| Sum formula | $\text{C}_5\text{O}_5\text{AlCl}_4\text{I}_2\text{TeRe}$ | $\text{C}_{12}\text{H}_{15}\text{N}_2\text{O}_4\text{I}_6\text{Te}_2\text{Re}$ | $\text{C}_3\text{O}_3\text{I}_7\text{Te}_3\text{Re}$ | $\text{C}_{26}\text{H}_{15}\text{N}_2\text{O}_{18}\text{Te}_6\text{Re}_5$ |
| Crystal system | Monoclinic | Monoclinic | Triclinic | Triclinic |
| Space group | $P2_1/c$ | $P2_1/c$ | $P\bar{1}$ | $P\bar{1}$ |
| Lattice parameters | $a = 1634.8(3)$ pm $b = 1728.7(3)$ pm $c = 1386.3(3)$ pm $\alpha = 90^\circ$ $\beta = 108.1(1)^\circ$ $\gamma = 90^\circ$ | $a = 970.9(2)$ pm $b = 1353.9(3)$ pm $c = 2297.6(6)$ pm $\alpha = 90^\circ$ $\beta = 108.6(1)^\circ$ $\gamma = 90^\circ$ | $a = 853.8(2)$ pm $b = 996.1(2)$ pm $c = 1322.9(2)$ pm $\alpha = 84.3(1)^\circ$ $\beta = 72.8(1)^\circ$ $\gamma = 86.0(1)^\circ$ | $a = 1152.1(2)$ pm $b = 1193.0(2)$ pm $c = 1925.5(4)$ pm $\alpha = 74.8(1)^\circ$ $\beta = 73.3(1)^\circ$ $\gamma = 64.6(1)^\circ$ |
| Cell volume | $V = 3724.1 \times 10^6$ pm ³ | $V = 2862.2 \times 10^6$ pm ³ | $V = 1068.6 \times 10^6$ pm ³ | $V = 2260.5 \times 10^6$ pm ³ |
| Formula units per cell | $Z = 8$ | $Z = 4$ | $Z = 2$ | $Z = 2$ |
| Calculated density | $\rho = 3.126$ g cm ⁻³ | $\rho = 3.374$ g cm ⁻³ | $\rho = 4.790$ g cm ⁻³ | $\rho = 3.438$ g cm ⁻³ |
| Measurement limits | $-22 \leq h \leq 22$, $-23 \leq k \leq 21$, $-18 \leq l \leq 19$ | $-13 \leq h \leq 13$, $-18 \leq k \leq 0$, $-31 \leq l \leq 12$ | $-11 \leq h \leq 10$, $-13 \leq k \leq 13$, $-18 \leq l \leq 18$ | $-15 \leq h \leq 15$, $-16 \leq k \leq 16$, $-26 \leq l \leq 26$ |
| Theta range for data collection | 3.5 to 58.8° | 3.0 to 58.5° | 4.1 to 58.6° | 3.8 to 58.8° |
| Linear absorption coefficient | $\mu = 12.00$ mm ⁻¹ | $\mu = 12.73$ mm ⁻¹ | $\mu = 19.81$ mm ⁻¹ | $\mu = 17.21$ mm ⁻¹ |
| Number of reflections | 17 854 (14 047 independent) | 32 083 (24 244 independent) | 10 458 (5317 independent) | 42 749 (12 235 independent) |
| Refinement method | Full-matrix least-squares on F^2 | Full-matrix least-squares on F^2 | Full-matrix least-squares on F^2 | Full-matrix least-squares on F^2 |
| Merging | $R_{\text{int}} = 0.149$ | $R_{\text{int}} = 0.072$ | $R_{\text{int}} = 0.058$ | $R_{\text{int}} = 0.107$ |
| Number of parameters | 343 | 264 | 154 | 515 |
| Residual electron density | 2.94 to -1.50 e ⁻ · 10 ⁻⁶ pm ⁻³ | 1.67 to -1.74 e ⁻ · 10 ⁻⁶ pm ⁻³ | 1.91 to -1.87 e ⁻ · 10 ⁻⁶ pm ⁻³ | 1.57 to -2.30 e ⁻ · 10 ⁻⁶ pm ⁻³ |
| Figures of merit | R_1 ($I \geq 4\sigma_1$) = 0.049 R_1 (all data) = 0.145 wR_2 (all data) = 0.096 GooF = 0.728 | R_1 ($I \geq 4\sigma_1$) = 0.032 R_1 (all data) = 0.041 wR_2 (all data) = 0.055 GooF = 0.956 | R_1 ($I \geq 4\sigma_1$) = 0.033 R_1 (all data) = 0.092 wR_2 (all data) = 0.055 GooF = 0.705 | R_1 ($I \geq 4\sigma_1$) = 0.038 R_1 (all data) = 0.12 wR_2 (all data) = 0.068 GooF = 0.731 |



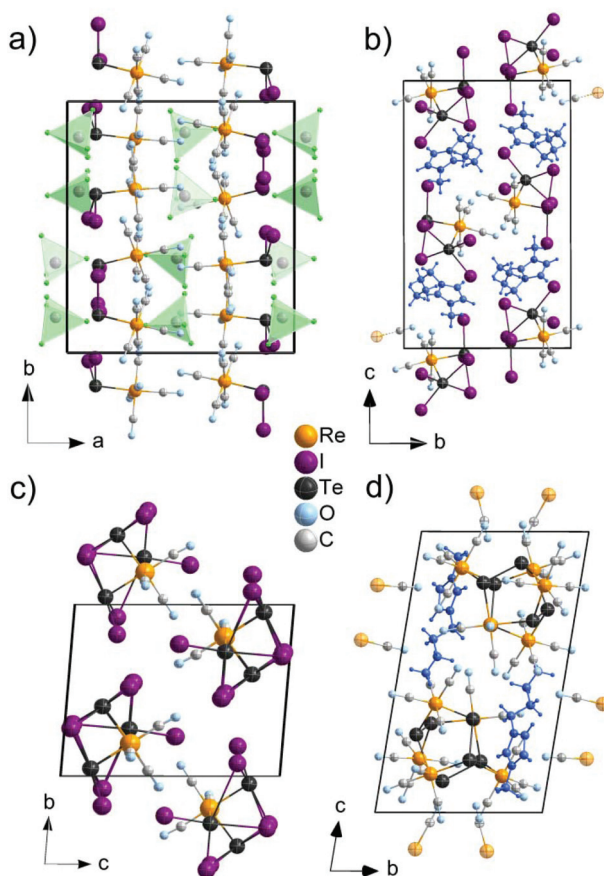
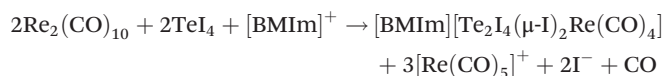


Fig. 1 Unit cells of the Te–Re carbonyls: (a) $[\text{TeI}_2\text{Re}(\text{CO})_5][\text{AlCl}_4]$ (1); (b) $[\text{BMIm}][\text{Te}_2\text{I}_4(\mu\text{-I})_2\text{Re}(\text{CO})_4]$ (2); (c) $\{\text{Te}_3\text{I}_2(\mu\text{-I})_3(\mu_3\text{-I})\}\text{Re}(\text{CO})_4$ (3); (d) $[\text{BMIm}][(\text{Te}_2)_3\{\text{Re}(\text{CO})_3\}_2\{\text{Re}(\text{CO})_4\}_3]$ (4) $[\text{BMIm}]^+$ displayed in dark blue, $[\text{AlCl}_4]^-$ displayed in light green.

The $[\text{TeI}_2\text{Re}(\text{CO})_5]^+$ cation, finally, exhibits an almost octahedrally coordinated Re atom with five carbonyl ligands and a tellurium atom (Fig. 1a). The Re–(CO) distances range from 193(2) (Re2–C10) to 206(2) pm (Re1–C3). These values relate to known Re–(CO) distances, *e.g.*, 192.9–200.7 pm in $\text{Re}_2(\text{CO})_{10}$.²⁴

$[\text{BMIm}][\text{Te}_2\text{I}_4(\mu\text{-I})_2\text{Re}(\text{CO})_4]$ (2)

$[\text{BMIm}][\text{Re}(\text{CO})_4\text{Te}_2\text{I}_2(\mu\text{-I})_2]$ was obtained with shiny black crystals by a similar reaction as 1, but with an increased amount of AlCl_3 , thus, with an $[\text{BMIm}]\text{Cl}:\text{AlCl}_3$ ratio of 1 : 2. The compound 2 crystallizes in the monoclinic space group $P2_1/c$ and consists of $[\text{BMIm}]^+$ cations, stemming from the IL, and $[\text{Te}_2\text{I}_4(\mu\text{-I})_2\text{Re}(\text{CO})_4]^-$ anions (Table 1 and Fig. 1b). The synthesis of 2 can be rationalized based on a similar redox reaction as for 1:



The $[\text{Te}_2\text{I}_4(\mu\text{-I})_2\text{Re}(\text{CO})_4]^-$ anion consists of a $\text{Te}_2\text{I}_4(\mu\text{-I})_2$ unit that is bonded to a $\text{Re}(\text{CO})_4^+$ group (Fig. 2b). With 276.7(1) (Te2–Re1) and 276.8(1) pm (Te1–Re1), the Te–Re distances are



Fig. 2 Structural units and connectivity of the Te–Re carbonyls with selected bond distances (in pm; Te–Te: black, Te–I: violet, Te–Re: yellow): (a) $[\text{TeI}_2\text{Re}(\text{CO})_5]^+$ cation in 1; (b) $[\text{Te}_2\text{I}_4(\mu\text{-I})_2\text{Re}(\text{CO})_4]^-$ anion in 2; (c, d) $\{\text{Te}_3\text{I}_2(\mu\text{-I})_3(\mu_3\text{-I})\}\text{Re}(\text{CO})_4$ (3) with structure of (c) rotated by 90° in (d); (e) Te_6Re_5 unit in 4; (f) $[(\text{Te}_2)_3\{\text{Re}(\text{CO})_3\}_2\{\text{Re}(\text{CO})_4\}_3]^-$ anion in 4.

Table 2 Comparison of selected distances in 1, 2, 3 and 4

| | Te–Re/pm | Te–Te/pm | Te–I/pm |
|---|-------------------|-------------------|---|
| 1 | 275.8(1)–275.9(1) | — | 269.4(2)–272.6(2) |
| 2 | 276.7(1)–276.8(1) | — | μ_1 : 275.9(1)–292.1(1) μ_2 : 300.3(1)–314.8(1) |
| 3 | 272.2(1)–274.0(1) | — | μ_1 : 276.2(2)–281.7(2) $\mu_{2/\text{short}}$: 274.4–276.0 $\mu_{2/\text{long}}$: 349.6–379.8 μ_3 : 318.7–331.5 |
| 4 | 276.3(1)–280.1(1) | 278.7(1)–279.5(1) | |

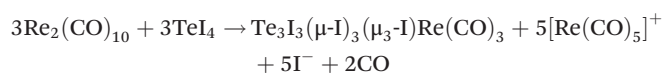
similar to 1 and compare with literature data as well (Table 2).^{12,14} Both Te atoms are interlinked by two I atoms with distances of 300.3(1) (Te1–I3) to 343.3(1) pm (Te2–I3). These distances are slightly longer compared to the bridging I atoms in the Te_4I_{16} building unit of TeI_4 (293.2–327.8 pm).²³ In addition, each Te atom is terminally coordinated to two I atoms. The respective Te–I distances (Te2–I1: 275.9(1), Te1–I6: 292.1(1) pm) are also in accordance with literature (Table 2).²³ Taken together, each Te atom is coordinated like a distorted square pyramid with four iodine atoms forming a square and one Re atom as top of the pyramid (Fig. 2b). Together with the



remaining lone pair a pseudo octahedron around Te is formed. The respective angles range from 83.4 (Re1–Te2–I3) to 99.7° (Re1–Te2–I2). Similar to **1**, Re is distorted octahedrally coordinated by four CO ligands and two Te atoms. The Re–(CO) distances (Re1–C4: 194.2(8) to Re1–C3: 201.8(7) pm) compare to those in **1** and Re₂(CO)₁₀.²⁴ Finally, the composition of **2** was validated by EDX analysis resulting a Te : I : Re ratio of 2.1 : 6 : 1.0 (scaled on I), which is well in accordance with the expectation (2 : 6 : 1).

Te₃I₃(μ-I)₃(μ₃-I)Re(CO)₃ (**3**)

Following the synthesis strategy of **1** and **2**, Te₃I₃(μ-I)₃(μ₃-I)Re(CO)₃ was obtained upon further increasing the amount of AlCl₃ resulting in a [BMIm]Cl : AlCl₃ ratio of 1 : 3. **3** formed shiny black crystals and crystallizes triclinically with the space group *P*₁ (Table 1 and Fig. 1c). EDX analysis confirms the chemical composition with a Te : I : Re of 2.7 : 7 : 0.9 (scaled on I, expected: 3 : 7 : 1). The synthesis can be ascribed to the following redox reaction:



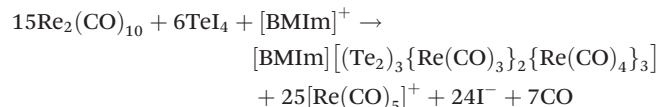
Te₃I₃(μ-I)₃(μ₃-I)Re(CO)₃ contains a Te₃I₃(μ-I)₃(μ₃-I) unit that is bond to a Re(CO)₃ unit (Fig. 2c and d). The Te–Re distances range from 272.2(1) (Te3–Re1) to 274.0(1) pm (Te2–Re1) and fit well to the distances observed in **1** and **2** (Table 2). Moreover, each Te atom is terminally bond to one iodine atom with comparable distances (Te3–I7: 276.2(2) to Te1–I5: 281.7(2) pm) as observed in **1**, **2** or the terminally bond I in TeI₄.²³ In addition, one iodine atom (I1) is μ₃-coordinated to all Te atoms (Fig. 2d). The observed distances of 318.7 (Te1–I1) to 331.5 (Te2–I1) pm are in agreement with Te–I distances of μ₃-coordinated iodine of the Te₄I₆ building unit in TeI₄ (319.8–324.1 pm).²³ Such μ₃-coordination of iodine to tellurium is yet only known for {(C₆H₅)TeI₄Te(C₆H₅)SCN₂H₄)}₂ and *o*-C₆H₄(CH₂TeMe₂)₂ as additional examples.²⁵ Finally, three iodine atoms (I2, I3, I4) bridge two Te atoms, leading to a Te₃I₃ ring (Fig. 2c). These μ₂-I atoms exhibit a short distance to one Te atom (274.4–276.0 pm) and comparably long distances to the other Te atom (349.6–379.8 pm) (Fig. 2d). Thus, bonding of iodine is significantly stronger to one of the Te atoms, which is similarly observed for Te–I distances of the dimer {(C₆H₅)TeI₄Te(C₆H₅)SCN₂H₄)}₂.²⁵

Re is again coordinated like a distorted octahedron. In **3**, however, Re is only bond by three carbonyl ligands in addition to three Te atoms (Fig. 2c and d). The Re–(CO) distances range from 192(6) (Re1–C2) to 195(1) pm (Re1–C1) and compare to those in **1**, **2** or Re₂(CO)₁₀.²⁴

[BMIm][[(Te₂)₃{Re(CO)₃}{Re(CO)₄}]₃] (**4**)

In difference to **1**, **2**, and **3**, the fourth Te–Re carbonyl compound [BMIm][[(Te₂)₃{Re(CO)₃}{Re(CO)₄}]₃ was prepared in [BMIm][OTf] as the IL instead of [BMIm]Cl/AlCl₃. In this regard, [BMIm][OTf] can be considered as non-acidic IL. Again, TeI₄ and Re₂(CO)₁₀ were used as starting materials and reacted at 130 °C. The synthesis of **4** can be ascribed to a

reduction of Te^{+IV} to Te^{-I} with oxidation of Re⁰ to Re^{+I} according to the following equation:



This sequence of reaction, in fact, compares to the reaction of TeI₄ and Mn₂(CO)₁₀ to [BMIm][[(Te₂)₃{Mn(CO)₃}{Mn(CO)₄}]₃, which we reported previously.¹⁰

4 crystallizes triclinically (space group *P*₁, Table 1) and contains the anion [[(Te₂)₃{Re(CO)₃}{Re(CO)₄}]₃⁻ and the IL-cation [BMIm]⁺ (Fig. 1d). The [[(Te₂)₃{Re(CO)₃}{Re(CO)₄}]₃⁻ anion exhibits three Te₂²⁻ ditelluride units and two Re(CO)₃⁺ fragments that establish a distorted heterocubane-like Te₆Re₂ unit with angles of 72.9(1) to 112.9(1)° (Fig. 2e and f). Three edges of this distorted cube are additionally bridged by Re(CO)₄⁺ fragments (Fig. 2f). The Te–Te distances in the Te₂²⁻ units with 278.7(1) (Te1–Te2) to 279.5(1) pm (Te5–Te6) can be considered as single bonds and fit with [Mn₄(CO)₁₃(Te₂)₃]²⁻ (272.3–277.7 pm)²⁶ or [[(Te₂)₃{Mn(CO)₃}]₂{Mn(CO)₄}]₃⁻ (277.0–278.3 pm)¹⁰ as reference compounds.

The intermolecular distances between different Te₂²⁻ groups in the heterocubane range from 381.1(1) (Te2–Te6) to 383.6(1) pm (Te1–Te4), which is still below the doubled van der Waals radius (418 pm),²⁷ indicating at least weak attractive interactions. Finally, Te₂²⁻ groups are bridged by Re(CO)₄⁺ units with Te–Re distances of 277.9(1) (Te2–Re3) to 280.1(2) pm (Te5–Re5), which is very similar to the respective distances in **1**, **2**, and **3** (276.3(1)–276.6(1) pm) (Table 1). Finally, EDX was again used to validate the chemical composition of **4**, resulting in a Re : Te ratio of 4.7 : 6 (scaled on Te), which fits with the expectation (5 : 6).

In regard of structure and connectivity of [[(Te₂)₃{Mn(CO)₃}]₂{Mn(CO)₄}]₃⁻, the Te₆Re₅ arrangement can be compared to the so-called ufosane anion P₁₁³⁻ (Fig. 2e).²⁸ Beside the similar shape, moreover, the electronic situation can be considered comparable. Thus, the electron deficient fragments Re(CO)₃⁺ (Re: 12e⁻) and Re(CO)₄⁺ (Re: 14e⁻) form three and two additional bonds. In contrast to P₁₁³⁻ with each phosphorus atom contributing one electron to each P–P bond, coordinative bonding is observed in **4** between the electron deficient Re(CO)₃⁺/Re(CO)₄⁺ fragments and the electron-rich Te₂²⁻ units.

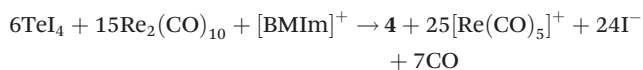
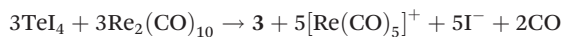
Comparison of synthesis conditions and compounds

The synthesis of the title compounds **1–4** can be obviously controlled by the conditions of the reaction. To avoid an unruled variation of conditions, several parameters were kept constant to allow direct comparison. Thus, temperature (130 °C), duration of heating (96 h) and the amount of TeI₄ (0.126 mmol) and Re₂(CO)₁₀ (1.718 mmol) with a Te : Re ratio of 1 : 27 were used to obtain all Te–Re carbonyls. In this regard, it needs to be noticed that the Te : Re ratio of **1**, **2** and **3** is identical (1 : 1) anyway. Excessive Re₂(CO)₁₀ is nevertheless essential due to the underlying redox reaction and the formation of [Re(CO)₅]⁺ as a by-product of all syntheses. In regard of the



stability of **1–4**, moreover, appreciable intermolecular interactions are lacking, and therefore, not decisive for the obtained compounds. Essential changes of the experimental conditions relate to the increasing amount of AlCl_3 , and thus, the increasing acidity of the IL in the direction **1** ($[\text{BMIm}]\text{Cl}:\text{AlCl}_3$ at 1:1) to **3** ($[\text{BMIm}]\text{Cl}:\text{AlCl}_3$ at 1:3) and the use of the acid–base neutral IL $[\text{BMIm}][\text{OTf}]$ for **4**.

The course of the reaction can be clearly arranged by focusing on the starting materials and the additional products besides the title compounds **1–4** as shown below:



In contrast to other metal carbonyls that we obtained by IL-based synthesis,^{9–11} only a minor amount of CO (in relation to the CO present in the starting materials) was released. Whereas the formation of, for instance, the Fe_4Sn_6 cluster in $[\{\text{Fe}(\text{CO})_3\}_4\{\text{SnI}_6\text{I}_4\}]^{2-}$ is clearly driven by CO release,⁹ the entropic effect is limited here. For **1–3**, in general, the number of remaining CO ligands decreases (5 in **1**, 4 in **2**, 3 in **3**), whereas the number of Te–Re is increased (1 in **1**, 2 in **2**, 3 in **3**). This variation can be directly related to the amount of AlCl_3 and the Lewis acidity of the applied IL. Since the formation of $[\text{AlCl}_4]^-$ is limited at $[\text{BMIm}]\text{Cl}:\text{AlCl}_3$ ratios <1 , excess AlCl_3 tends to coordinate I^- stemming from TeI_4 and thereby supports the formation of Te–Re bonds and the occurrence of μ_2 - or μ_3 -bridged I atoms. Finally, it needs to be noticed that the solubility of TeI_4 and $\text{Re}_2(\text{CO})_{10}$ is poor in $[\text{BMIm}]\text{Cl}/\text{AlCl}_3$, especially at 1:1 ratio. Thus, excess AlCl_3 not only influences the type of product, but also supports the solubility of the starting materials. $[\text{BMIm}][\text{OTf}]$ used for the synthesis of **4** is much less polar than $[\text{BMIm}]\text{Cl}/\text{AlCl}_3$, resulting in a good solubility of TeI_4 and $\text{Re}_2(\text{CO})_{10}$. The higher concentration of dissolved reactants, on the one hand, obviously supports the redox reaction and results in the oxidation of rhenium with formation of $[\text{Re}^{\text{VI}}(\text{CO})_5]^+$ as observed for all title compounds. Whereas Te^{IV} was reduced to Te^{III} in the case of **1–3**, the reduction proceeds to Te^{II} only for **4**, resulting in Te–Te bonds and the total absence of Te–I bonds.

For further characterization and comparison of the Te–Re carbonyl compounds **1–4**, Fourier-transformed (FT-IR) spectroscopy and thermogravimetry (TG) were performed. According to FT-IR, all compounds show characteristic CO vibrations (Fig. 3), which can be assigned to strong $\nu(\text{C}=\text{O})$ and weaker $\delta(\text{Re}-\text{C}=\text{O})$ vibrations.²⁹ By tendency, the C=O vibration is shifted to higher wavenumbers with increasing number of electronegative Te atoms coordinated to rhenium (**1** \rightarrow **2** \rightarrow **3/4**) (Table 3). Moreover, the CO vibrations broaden

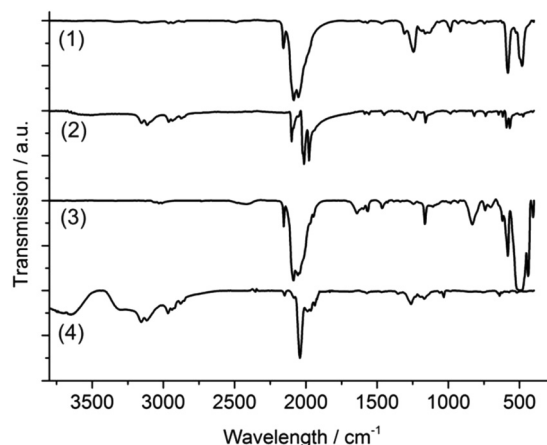


Fig. 3 FT-IR spectra of the Te–Re carbonyl compounds **1**, **2**, **3**, and **4**.

Table 3 Comparison of carbonyl vibrations of **1**, **2**, **3**, and **4** with literature data (strong vibrations in bold letters)

| Compound | Vibration/cm ⁻¹ |
|---|--|
| 1 | 2185, 2085 , 2053 |
| 2 | 2101 , 2023, 2013 , 1978 |
| 3 | 2155, 2087 , 2057 , 2043 , 1946 |
| 4 | 2150, 2083, 2042 , 1991, 1966, 1937 |
| $\text{Re}_2(\text{CO})_{10}$ ²⁴ | 2070, 2014, 2003, 1976 |
| $\text{Re}(\text{CO})_5\text{Cl}$ ²⁹ | 2156, 2056, 1987 |

with the number of non-symmetry equivalent CO groups (**1** \rightarrow **2/3** \rightarrow **4**). Additional vibrations of **2** and **4** stem from the $[\text{BMIm}]^+$ cation ($\nu(\text{C}-\text{H})$: 3150–2900 cm^{-1} , fingerprint area: 1600–1100 cm^{-1} , Fig. 3). Moreover, certain vibrations relate to the inert oil (perfluoroalkylether), in which the crystals were embedded for stabilization (1308, 1244, 1185, 1162, 985 cm^{-1}). The observed CO vibrations are well in agreement with terminal carbonyl ligands as observed, for instance, in $\text{Re}_2(\text{CO})_{10}$ or $\text{Re}(\text{CO})_5\text{Cl}$ (Table 3).^{24,29}

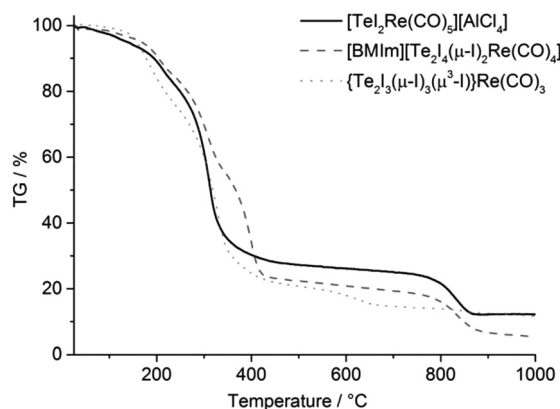
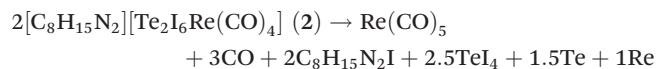
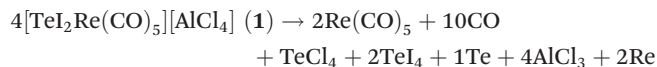


Fig. 4 Thermogravimetric analysis of the Te–Re carbonyl compounds **1**, **2** and **3**.



TG was used to compare the thermal stability of the Te–Re carbonyls **1**, **2** and **3** (Fig. 4). Since **4** was only obtained with minor quantities, TG of this phase could not be performed. Generally, all compounds show two-step decomposition with slow release starting already at room temperature. At temperatures higher than 180 °C, the decomposition becomes very fast and results in a major release (70–80 wt%) of gaseous compounds up to 450 °C. A second decomposition step (about 15 wt%) occurred for **1** and **2** at 750–850 °C (Fig. 4). Although the thermal decomposition is generally very similar, the neutral compound **3** shows the lowest decomposition temperature, which can be ascribed to the lacking lattice energy in comparison to the ionic compounds **1** and **2**. All in all, the thermal decomposition can be ascribed to the following reactions:



Thus, elemental rhenium remains as thermal residue, which is in accordance with a black, metallic film on the crucible surface. Whereas the first massive decomposition step can be explained by more-or-less simultaneous release of $\text{Re}(\text{CO})_5$, CO, TeCl_4 , TeI_4 and $\text{C}_8\text{H}_{15}\text{N}_2\text{I}$, the second decomposition step relates to the evaporation of Al_2Cl_6 for **1** and the evaporation of tellurium for **2**.

Conclusions

The four novel Te–Re carbonyls $[\text{TeI}_2\text{Re}(\text{CO})_5][\text{AlCl}_4]$ (**1**), $[\text{BMIm}][\text{Re}(\text{CO})_4\text{Te}_2\text{I}_4(\mu\text{-I})_2]$ (**2**), $\text{Re}(\text{CO})_3\{\text{Te}_3\text{I}_2(\mu\text{-I})_3(\mu_3\text{-I})\}$ (**3**) and $[\text{BMIm}][(\text{Te}_2)_3\{\text{Re}(\text{CO})_3\}_2\{\text{Re}(\text{CO})_4\}_3]$ (**4**) are presented for the first time. The title compounds were prepared by reaction of TeI_4 and $\text{Re}_2(\text{CO})_{10}$ in $[\text{BMIm}]\text{Cl}/\text{AlCl}_3$ or $[\text{BMIm}][\text{OTf}]$. All of them turned out as highly reactive and sensitive to air and moisture, which can be ascribed to the absence of stabilizing alkyl and aryl ligands.

All title compounds were characterized *via* single-crystal structure analysis, EDX and FT-IR spectroscopy. Thus, **1** contains a $[\text{TeI}_2\text{Re}(\text{CO})_5]^+$ cation, **2** the anion $[\text{Te}_2\text{I}_4(\mu\text{-I})_2\text{Re}(\text{CO})_4]^-$. **3** exhibits a remarkable Te_3I_3 ring and μ_3 -coordinating iodine. **4** contains the ufosan-like anion $[(\text{Te}_2)_3\{\text{Re}(\text{CO})_3\}_2\{\text{Re}(\text{CO})_4\}_3]^-$ with three Te_2^{2-} and two $\text{Re}(\text{CO})_3^+$ units that establish a distorted heterocubane-like cage.

IL-based synthesis turned out as a versatile strategy to obtain reactive metal carbonyl compounds. The formation of the compounds **1–4** can be steered by the type and acidity of the IL. Thus, depending on the amount of AlCl_3 applied in the synthesis, the number of CO ligands decreases from 5 (**1**) *via* **4** (**2**) to 3 (**3**) and the number of Te–Re bonds increases from

1 (**1**) *via* **2** (**2**) to 3 (**3**). In addition, **1** exhibits only terminally bond I atoms, **2** bridging (μ_2) and terminally coordinated I atoms and **3** bridging (μ_2 , μ_3) and terminally coordinated I atoms. Hence, the connectivity of iodine can be as well related to the amount of AlCl_3 and the acidity of the IL. In the case of the acid–base neutral IL $[\text{BMIm}][\text{OTf}]$ for the synthesis of **4**, the significantly increased solubility of TeI_4 and $\text{Re}_2(\text{CO})_{10}$ is decisive and results in a different redox reaction with Te^{+IV} reduced to Te^{-I} , whereas the reduction is limited to Te^{+II} for **1–3**. Taken together, IL-based synthesis allows preparing four different Te–Re carbonyls in the system $\text{TeI}_4/\text{Re}_2(\text{CO})_{10}$ with good control due to specific experimental conditions. This observation leaves plenty of room for reaction control and the realization of numerous novel compounds in other systems.

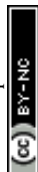
Experimental

Synthesis

General. All reactions and sample handling were carried out under dried argon atmosphere using standard Schlenk techniques or glove boxes. Reactions were performed in Schlenk flasks and glass ampoules that were evacuated ($p < 10^{-3}$ mbar), heated and flashed with argon three times prior to use. The starting materials TeI_4 (99.99%, ABCR), $\text{Re}_2(\text{CO})_{10}$ (99%, ABCR), AlCl_3 (99.99%, Sigma-Aldrich) and $[\text{BMIm}][\text{OTf}]$ (Merck, high purity) were used as received. $[\text{BMIm}]\text{Cl}$ (99%, Iolitec) was dried under reduced pressure (10^{-3} mbar) at 150 °C for 48 h. All compounds were handled and stored in argon-filled glove boxes (MBraun Unilab, $c(\text{O}_2, \text{H}_2\text{O}) < 0.1$ ppm). Regarding the stability of all title compounds, it needs to be noticed that slow decomposition occurred due to CO loss when removing the compound and single crystals from the mother lye.

$[\text{TeI}_2\text{Re}(\text{CO})_5][\text{AlCl}_4]$ (**1**). 80 mg (0.126 mmol) of TeI_4 , 82.2 mg (0.126 mmol) of $\text{Re}_2(\text{CO})_{10}$, 300 mg (1.718 mmol) of $[\text{BMIm}]\text{Cl}$ and 256.8 mg (1.718 mmol) of AlCl_3 were heated under argon in a sealed glass ampoule for 96 h at 130 °C. After cooling to room temperature with a rate of 1 K h^{-1} , **1** was obtained as red crystals together with minor amounts of colourless crystals of excess $\text{Re}_2(\text{CO})_{10}$ and yellow needles of $[\{\text{Re}(\text{CO})_5\}_2\text{I}][\text{Al}_2\text{Cl}_7]$. Reducing the amount of $\text{Re}_2(\text{CO})_{10}$ (down to 0.063 mmol), however, resulted in a lower crystal quality and, if further reduced, to any crystallization at all. **1** is highly sensitive to air and moisture and needs to be handled under inert conditions. Since **1** could not be obtained phase-pure (yield of about 20%), the crystals for characterization were manually separated by crystal picking. From all title compounds, **1** is most sensitive, which is in accordance with the high content of CO per formula unit. This situation also limits the quality of single crystals.

$[\text{BMIm}][\text{Te}_2\text{I}_4(\mu\text{-I})_2\text{Re}(\text{CO})_4]$ (**2**). 80 mg (0.126 mmol) of TeI_4 , 82.2 mg (0.126 mmol) of $\text{Re}_2(\text{CO})_{10}$, 300 mg (1.718 mmol) of $[\text{BMIm}]\text{Cl}$ and 513.5 mg (3.436 mmol) of AlCl_3 were heated under argon in a sealed glass ampoule for 96 h at 130 °C. After cooling to room temperature with a rate of $1 \text{ }^\circ\text{C h}^{-1}$, **2** was



obtained as shiny black crystals together with colorless crystals of excess $\text{Re}_2(\text{CO})_{10}$. After filtration, $\text{Re}_2(\text{CO})_{10}$ can be dissolved in CH_2Cl_2 yielding phase pure **2** with a yield of about 30%. **2** is highly sensitive to moisture.

In alternative to the above recipe with $[\text{BMIm}]\text{Cl}$ and AlCl_3 , **2** can be also prepared using $[\text{BMIm}][\text{OTf}]$ as the IL. This route, however, resulted in a mixture of **2** and **4**, whereas the reaction with $[\text{BMIm}]\text{Cl}$ and AlCl_3 as IL yields **2** as sole Te–Re compound.

$\{\text{Te}_3\text{I}_2(\mu\text{-I})_3(\mu_3\text{-I})\}\text{Re}(\text{CO})_3$ (**3**). 80 mg (0.126 mmol) of TeI_4 , 82.2 mg (0.126 mmol) of $\text{Re}_2(\text{CO})_{10}$, 300 mg (1.718 mmol) of $[\text{BMIm}]\text{Cl}$ and 770.4 mg (5.154 mmol) of AlCl_3 were heated under argon in a sealed glass ampoule for 96 h at 130 °C. After cooling to room temperature with a rate of 1 °C h^{-1} , **3** was obtained with about 20% of yield as dark red, almost black crystals as the main phase together with few colorless crystals of excess $\text{Re}_2(\text{CO})_{10}$. Again, a reduction of $\text{Re}_2(\text{CO})_{10}$ (down to 0.063 mmol) in the synthesis did neither lead to a phase pure product nor to any crystallization at all. **3** is highly sensitive to oxygen and moisture as well.

$[\text{BMIm}][(\text{Te}_2)_3\{\text{Re}(\text{CO})_3\}_2\{\text{Re}(\text{CO})_4\}_3]$ (**4**). 80 mg (0.126 mmol) of TeI_4 , 82.2 mg (0.126 mmol) of $\text{Re}_2(\text{CO})_{10}$ were dissolved in 1 mL $[\text{BMIm}][\text{OTf}]$ and heated under argon in a sealed glass ampoule for 96 h at 130 °C. After cooling to room temperature with a rate of 1 °C h^{-1} , **4** was obtained as red crystals with about 5% of yield as a minor phase together with black crystals of **2** as the main phase. **4** is also highly sensitive to oxygen and moisture. Since **4** could not be obtained as a pure phase, crystals for characterization were separated manually by crystal picking.

Analytical equipment

Single-crystal X-ray structure analysis. For single crystal structure analysis, suitable crystals were selected manually, covered by inert-oil (perfluoropolyalkylether, ABCR), and placed in a glass capillary (Hilgenberg) that was sealed immediately. Data collection was performed at 200 K on an IPDS II image-plate diffractometer (Stoe, Darmstadt) using $\text{Mo-K}\alpha$ radiation ($\lambda = 0.71073$ Å, graphite monochromator). Data reduction and numerical absorption correction were conducted by the X-Area software package (version 1.26).³⁰ Due to the high sensitivity of the title compounds and the resulting limited crystal quality (especially for **1**), proper correction of absorption effects was difficult. Space group determination based on systematic absence of reflections, structure solution by direct methods and refinement were performed by XPREP and SHELXTL (version 6.14, SHELXS-97).³¹ All non-hydrogen atoms were refined anisotropically. Detailed information on crystal data and structure refinement is listed in Table 1. DIAMOND was used for all illustrations.³² Further details of the crystal structure investigation may be obtained from the joint CCDC/FIZ Karlsruhe deposition service on quoting the depository numbers CCDC 1913799–1913802.‡

Fourier-transformed infrared (FT-IR) spectra were recorded on a Bruker Vertex 70 FT-IR spectrometer (Bruker). The samples were measured as pellets in KBr. Thus, 300 mg of dried KBr

and 0.5–1.0 mg of the sample were carefully pestled together and pressed to a thin pellet.

Thermogravimetry (TG) was carried out with a Netzsch STA 449 F3 Jupiter device using $\alpha\text{-Al}_2\text{O}_3$ as crucible material and reference. Buoyancy effects were corrected by baseline subtraction of a blank measurement. The samples were measured under dried nitrogen up to 800 °C with a heating rate of 10 K min^{-1} .

Energy dispersive X-ray (EDX) analysis was performed using an Ametek EDAX mounted on a Zeiss SEM Supra 35 VP scanning electron microscope. The samples were prepared in the glove-box by selecting single crystals that were fixed on a conductive carbon pad on an aluminum sample holder. The samples were handled under inert conditions during transport and sample preparation.

Conflicts of interest

There are no conflicts to declare.

Acknowledgements

The authors thank the Deutsche Forschungsgemeinschaft (DFG) for funding in the Priority Program SPP1708 “*Synthesis near room temperature*”.

Notes and references

- P. Wasserscheid and T. Welton, *Ionic Liquids in Synthesis*, Wiley-VCH, Weinheim, 2008.
- D. Freudenmann, S. Wolf, M. Wolff and C. Feldmann, *Angew. Chem., Int. Ed.*, 2011, **50**, 11050 (Review).
- E. Ahmed and M. Ruck, *Dalton Trans.*, 2011, **40**, 9347 (Review).
- M. F. Groh, A. Wolff, M. A. Grasser and M. Ruck, *Int. J. Mol. Sci.*, 2016, **17**, 1452.
- A. M. Guloy, R. Ramlau, Z. Tang, W. Schnelle, M. Baitinger and Y. Grin, *Nature*, 2006, **443**, 320.
- (a) P. Braunstein, L. A. Oro and P. R. Raithby, *Metal Clusters in Chemistry*, Wiley-VCH, Weinheim, 2008; (b) G. Frenking and N. Froehlich, *Chem. Rev.*, 2000, **100**, 717.
- (a) M. F. Groh, A. Isaeva, U. Müller, P. Gebauer, M. Knies and M. Ruck, *Eur. J. Inorg. Chem.*, 2016, **2016**, 880; (b) M. F. Groh, J. Breternitz, E. Ahmed, A. Isaeva, A. Efimova, P. Schmidt and M. Ruck, *Z. Anorg. Allg. Chem.*, 2015, **641**, 388; (c) E. Ahmed, A. Isaeva, A. Fiedler, M. Haft and M. Ruck, *Chem. – Eur. J.*, 2011, **17**, 6847; (d) E. Ahmed, J. Breternitz, M. F. Groh, A. Isaeva and M. Ruck, *Eur. J. Inorg. Chem.*, 2014, **2014**, 3037.
- (a) S. Wolf and C. Feldmann, *Z. Anorg. Allg. Chem.*, 2017, **643**, 25; (b) S. Wolf, W. Klopper and C. Feldmann, *Chem. Commun.*, 2018, **54**, 1217.
- S. Wolf, F. Winter, R. Pöttgen, N. Middendorf, W. Klopper and C. Feldmann, *Chem. – Eur. J.*, 2012, **18**, 13600.



- 10 S. Wolf and C. Feldmann, *Z. Anorg. Allg. Chem.*, 2012, **638**, 1787.
- 11 S. Wolf, K. Reiter, F. Weigend, W. Klopper and C. Feldmann, *Inorg. Chem.*, 2015, **54**, 3989.
- 12 Y. V. Torubaev, A. A. Pasynskii and P. Mathur, *Russ. J. Coord. Chem.*, 2009, **35**, 807.
- 13 (a) P. Jeitner and W. Winder, *Inorg. Chim. Acta*, 1987, **134**, 201; (b) W. Hieber, W. Opavsky and W. Rohm, *Chem. Ber.*, 1968, **101**, 2244; (c) F. Calderazzo, D. Vitali, R. Poli, J. L. Atwood, R. D. Rogers, J. M. Cummings and I. Bernal, *J. Chem. Soc., Dalton Trans.*, 1981, 1004.
- 14 W. Levason, S. D. Orchard and G. Reid, *Organometallics*, 1999, **18**, 1275.
- 15 J. Muthukumar, M. Kannan, A. Vanitha, B. Manimaran and R. Krishnaa, *Acta Crystallogr., Sect. E: Struct. Rep. Online*, 2010, **66**, m558.
- 16 W. Beck, W. Sacher and U. Nagel, *Angew. Chem.*, 1986, **98**, 280.
- 17 A. A. Pasynskii, S. S. Shapovalov, I. V. Skabitsky, O. G. Ikhonova and T. A. Krishtop, *Russ. J. Coord. Chem.*, 2015, **41**, 75.
- 18 Y. V. Mironov, A. V. Virovets, W. S. Sheldrick and V. E. Fedorov, *Polyhedron*, 2001, **20**, 969.
- 19 G.-X. Jin, Y. Arikawa and K. Tatsumi, *J. Am. Chem. Soc.*, 2001, **123**, 735.
- 20 Y. V. Mironov, J. A. Cody, T. E. Albrecht-Schmitt and J. A. Ibers, *J. Am. Chem. Soc.*, 1997, **119**, 493.
- 21 V. P. Fedin, V. E. Fedorov, H. Imoto and T. Saito, *Polyhedron*, 1997, **16**, 1615.
- 22 R. Mews, *Angew. Chem.*, 1976, **88**, 28.
- 23 (a) V. Paulat and B. Krebs, *Angew. Chem.*, 1976, **88**, 28; (b) B. Krebs and V. Paulat, *Acta Crystallogr., Sect. B: Struct. Crystallogr. Cryst. Chem.*, 1976, **32**, 1470.
- 24 M. R. Churchill, K. N. Amoh and H. J. Wasserman, *Inorg. Chem.*, 1981, **20**, 1609.
- 25 (a) E. Schulz Lang, G. A. Casagrande, G. Manzoni de Oliveira, G. N. Ledesma, S. S. Lemos, E. E. Castellano and U. Abram, *Eur. J. Inorg. Chem.*, 2006, 958; (b) N. J. Hill, W. Levason, G. Reid and A. J. Ward, *J. Organomet. Chem.*, 2002, **642**, 186.
- 26 (a) M. A. El-Sayed and H. D. Kaesz, *J. Mol. Spectrosc.*, 1962, **9**, 310; (b) E. W. Abel, G. B. Hargreaves and G. Wilkinson, *J. Chem. Soc.*, 1958, 3149; (c) S. D. Huang, C. P. Lai and C. L. Barnes, *Angew. Chem., Int. Ed. Engl.*, 1997, **36**, 1854.
- 27 M. Mantina, A. C. Chamberlin, R. Valero, C. J. Cramer and D. G. Truhlar, *J. Phys. Chem. A*, 2009, **113**, 5806.
- 28 (a) W. Wichelhaus and H. G. von Schnering, *Naturwissenschaften*, 1973, **60**, 104; (b) H. G. von Schnering and W. Hönle, *Chem. Rev.*, 1988, 243.
- 29 N. Fliteroft, D. K. Huggins and H. D. Kaesz, *Inorg. Chem.*, 1964, **3**, 1123.
- 30 X-RED32, *Data Reduction Program, Version 1.01*, Stoe, Darmstadt, 2001.
- 31 (a) *SHELXTL – Structure Solution and Refinement Package, Version 5.1*, Bruker AXS, Karlsruhe, 1998; (b) G. M. Sheldrick, *Acta Crystallogr., Sect. A: Found. Crystallogr.*, 2008, **64**, 112.
- 32 *DIAMOND Version 4.2.2. – Crystal and Molecular Structure Visualization*, Crystal Impact GbR, Bonn, 2016.

